Active Cancellation of Periodic DM EMI at the Input of a GaN Motor Inverter by Injecting Synthesized and Synchronized Signals

Andreas Bendicks, Michael Gerten, Stephan Frei
On-board Systems Lab
TU Dortmund University
Dortmund, Germany
andreas.bendicks@tu-dortmund.de

***Abstract*—Active cancellation is a promising solution to reduce the size of passive filter components. Considering power electronic systems in stationary operation and with periodic control signals, the disturbances consist of stable harmonics that can be individually suppressed by destructive sine waves. These sine waves can be superposed to create a synthesized broadband cancellation signal that must be injected in synchronicity with the operation of the power electronic system. Since bothersome effects (like time constants or delay times) can be compensated by appropriate amplitudes and phases of the cancelling sine waves, the active cancellation system can achieve high EMI reductions in a wide frequency range. In this work, the method is applied to a motor inverter with a very large number of differential mode (DM) harmonics. The characteristics of the disturbances are discussed and the challenges for the active EMI cancellation system are elaborated. A suitable method for the determination and generation of the cancellation signal is introduced. This method is applied to a GaN inverter with a synchronous machine in the frequency range from 50 kHz to 30 MHz. The EMI suppression is evaluated by average and peak measurements with an EMI test receiver. The power of the generated cancellation signal is estimated.**

***Keywords*—Motor inverter; periodic EMI; active cancellation; synthesized signals; harmonics**

I. Introduction

Power electronic systems tend to be considerable sources of **e**lectro**m**agnetic **i**nterferences (EMI) due to the high-frequency switching of power transistors. To comply with international standards on **e**lectro**m**agnetic **c**ompatibility (EMC), e.g. CISPR 25 in automotive [1], the conducted EMI is commonly reduced by the application of passive filters that are often bulky, heavy and expensive. To resolve this issue, active cancellation techniques can be applied that aim at a destructive interference between noise and anti-noise [2]. This strategy is commonly applied in acoustics and successively in EMC.

In EMC, **a**ctive **E**MI **f**ilters (AEFs) have been developed in, e.g., [3]-[6] and further analyzed and systemized in, e.g., [7] and [8]. Like passive EMI filters, AEFs are connected between the EMI source and EMI victim. These systems use analog (or digital, e.g. [9] and [10]) circuitry to actively inject cancellation signals for a destructive interference with the disturbances. The cancellation signal is directly generated from a measured quantity by a feedback or a feedforward approach. As described in [7] and [8], the performance of analog AEFs mainly depends on the ratios of the amplifier's frequency-dependent gain and the EMI source's and victim's impedances. In general, high EMI reductions require high amplifier gains. Since the high-frequency amplifier gains are usually limited by internal (and maybe also external) time constants, AEFs are generally more effective for lower frequencies. Further limitations may result from the additional components for the stabilization of feedback AEFs [7], deviations in the inversion of feedforward AEFs, time constants due to the injecting and sensing circuits, delay times due to the signal propagation and delay times due to the signal processing in digital variants.

Analog AEFs for the input of motor inverters are mostly discussed for **c**ommon **m**ode (CM) EMI, e.g., [11]-[14]. In [11], the EMI is reduced by 20 dB between 250 kHz and 6 MHz. In [12], the EMI is reduced by over 35 dB between 100 and 600 kHz. For lower and higher frequencies, the EMI reduction diminishes in both publications. In [13], there is an EMI reduction of approximately 38 dB at 12 kHz. The AEF's performance declines for higher frequencies and has basically no effect at 3 MHz anymore. In [14], the EMI between 150 kHz and 300 kHz is suppressed by approximately 10 dB. There is no effect for frequencies above 500 kHz. These results also show that AEFs are most effective for lower frequencies.

To resolve the limitations of AEFs, the feedback or feedforward approaches for signal generation must be avoided. To do so, the cancellation signal can be artificially synthesized if the disturbances are known in advance, as shown in, e.g., [15]. Obviously, it is no trivial task to synthesize a complex broadband cancellation signal. However, considering (quasi-) periodic EMI, the disturbing spectrum only consists of discrete harmonics. So, it is feasible to generate a broadband cancellation signal from individual cancelling sine waves. By adjusting the respective amplitudes and phases, many bothersome effects (like time constants or delay times) can be compensated. To maintain a destructive interference, the artificially synthesized cancellation signal must be injected in synchronicity to the EMI.

This concept has already shown very promising results for DC-to-DC converters with EMI reductions of, e.g., 60 dB for 300 kHz and 40 dB for 30 MHz [16]. In [17], the method has been applied for the first time to the **d**ifferential **m**ode (DM) EMI at the input of a stationary operating motor inverter with a switching frequency of 100 kHz. The EMI could be suppressed by approximately 40 dB for the switching harmonics at 200, 300, 400 and 500 kHz. In [17], the suppressible frequency range was limited by the finite memory depth of the used **a**rbitrary **w**aveform **g**enerator (AWG). In this work, the frequency range of the active cancellation system is significantly increased by utilizing a new and optimized test setup that enables an active EMI suppression from 50 kHz to 30 MHz.

At first, the application is presented, and the active EMI cancellation system is introduced. The relevant signals are described by two Fourier series and a transfer function. From

978-1-7281-5579-1/20/$31.00 ©2020 IEEE

this description, the ideal cancellation signal is calculated. Although the cancellation signal can conveniently be synthesized from sine waves (assuming periodic disturbances), this process is not trivial since a very large number of cancelling sine waves must be found with high precision. To resolve this issue, a digital cancellation system using a DAC, an ADC, two memory units and a signal processor is proposed. A suitable method to determine and generate the required cancellation signal is presented. In this paper, the cancellation system is realized by using laboratory test equipment, i.e., an AWG, an oscilloscope and a PC. It is applied to the input of a 48 V motor inverter with GaN power transistors. The test setup is described, and the measurement results for the average and peak emissions are discussed. The power of the generated cancellation signal is estimated. The work is closed by a conclusion and an outlook.

II. Introduction of the Application and the Active EMI Cancellation System

In this chapter, the application and the active EMI cancellation system are introduced. At first, a motor inverter in a standard test setup is presented. Afterward, the required components for the cancellation system are added and explained.

A. Motor Inverter in Standard Test Setup

The considered setup of the motor inverter system is depicted in Fig. 1. To drive the motor, the inverter uses three half bridges to generate a three-phase voltage system from the DC supply voltage V_{supply}. At the input, the motor inverter has a large input capacitance C_{in} that usually consists of large electrolytic and small ceramic capacitors. In reference to the automotive standard CISPR 25 [1], an **a**rtificial **n**etwork (AN) is used to measure the conducted voltage disturbances $V_{\text{EMI}}^{@\text{AN}}(f)$ that origin from the switching of the motor inverter. Since the system uses the reference ground plane as return conductor, there are only DM disturbances against ground.

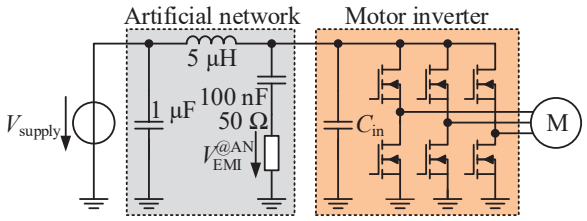

Fig. 1: Setup of the considered system.

B. Insertion of the Active Cancellation System

To suppress the conducted EMI at the input of the motor inverter, an active EMI cancellation system is introduced as depicted in Fig. 2. The motor inverter and the cancellation system form the **d**evice **u**nder **t**est (DUT). To eliminate the conducted EMI at the input side (that is measured by the AN), the interface port between the DUT and the AN must be free of disturbances.

The active EMI cancellation system uses a cancellation source with the voltage $V_{\text{anti}}(f)$ and the internal impedance $Z_{\text{anti}}(f)$. The determination and generation of the required cancellation signal will be described in a later section. The cancellation source is coupled via an injecting circuit to the overall system. This circuit should pass the high-frequency anti-EMI and reject the possibly large operating voltages and currents of the motor inverter that could otherwise destroy the cancellation source. EMI and anti-EMI propagate through the system and superpose each other. At the interface port, these

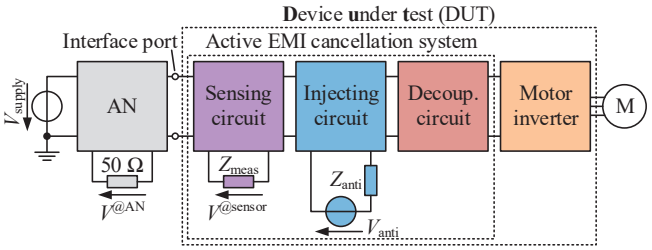

Fig. 2: Insertion of the injecting, sensing and decoupling circuit.

two signals must cancel each other out. The success of the active cancellation can be evaluated by using a sensor that is directly placed at the interface port. Like the injecting circuit, this circuit should also pass the high-frequency signals in the considered frequency range and reject the potentially harmful operating voltages and currents.

For an efficient cancellation system, the cancellation source should ideally be directly coupled to the interface port without a significant insertion loss. Depending on the topology of the injecting circuit and the impedance ratios of the EMI source (motor inverter) and EMI victim (AN), the cancellation signal may be diverted away from the EMI victim and towards the EMI source. In this case, the cancellation source may need to generate very large signals to still fulfill its requirement at the interface port. To avoid unnecessarily large signals, the injecting circuit can be decoupled from the EMI source by an appropriate decoupling circuit.

III. Determination of the Ideal Cancellation Signal

In this chapter, the ideal cancellation signal $v_{\text{anti}}(t)$ is determined that can completely cancel out the EMI of a motor inverter in stationary operation with periodic control signals. To do so, the EMI and the generated anti-EMI are represented by Fourier series. The propagation of the anti-EMI to the sensor is described by using a transfer function in frequency domain. The superposition of EMI and anti-EMI is calculated at the sensor. From this description, the ideal complex amplitudes for the anti-EMI can conveniently be found.

A. Description of the EMI at the Sensor

The half bridges of the motor inverter operate at a **sw**itching frequency f_{sw} to generate the three-phase voltage system with the frequency f_{elec} (**elec**tric). In this work, the system is assumed to be in stationary operation (i.e. constant load and supply conditions) with periodic control signals that repeat themselves with the fundamental period $T_{\text{elec}} = 1/f_{\text{elec}}$ of the three-phase system. If the three-phase system were completely symmetric, the disturbances would repeat themselves after $T_{\text{elec}}/3$ due to the 120° phase shift. Since a complete symmetry is usually not given, the disturbances can be expected to repeat themselves with T_{elec}. The EMI of the inverter may also change depending on the position of the motor's rotor [17]. Due to the pole pair number p, the rotor requires the time $T_0 = pT_{\text{elec}}$ to do a complete mechanical turn of 360°. Therefore, the EMI can be expected to repeat itself with the period T_0 and the frequency $f_0 = 1/T_0$. The EMI will propagate through the system and generate a voltage drop $v_{\text{EMI}}^{@\text{sensor}}(t)$ at the sensor. Given that the signal repeats itself periodically, it can be described by a Fourier series according to (1) [18]. The signal consists of harmonics with a spacing of f_0. This is the signal that must be cancelled out.

B. Description of the Anti-EMI at the Sensor

In analogy to (1), the anti-EMI $v_{\text{anti}}(t)$ can also be described by a Fourier series with the spacing of f_0 according

$$v_{\mathrm{EMI}}^{@\mathrm{sensor}}(t) = V_{\mathrm{EMI}}^{@\mathrm{sensor}}(0) + \sum_{k=1}^{\infty} 2\left|V_{\mathrm{EMI}}^{@\mathrm{sensor}}(kf_0)\right| \cos\left(2\pi k f_0 t + \angle V_{\mathrm{EMI}}^{@\mathrm{sensor}}(kf_0)\right) \quad (1)$$

$$v_{\mathrm{anti}}(t) = V_{\mathrm{anti}}(0) + \sum_{k=1}^{\infty} 2|V_{\mathrm{anti}}(kf_0)| \cos\left(2\pi k f_0 t + \angle V_{\mathrm{anti}}(kf_0)\right) \quad (2)$$

to (2). This signal will propagate through the overall system and superpose itself with the EMI.

To determine the effect of the anti-EMI on the sensor signal $v_{\mathrm{anti}}^{@\mathrm{sensor}}(t)$, the propagation from the cancellation source to the sensor must be described. This can conveniently be done in frequency domain by using a complex transfer function $H_{\mathrm{anti}}^{\rightarrow\mathrm{sensor}}(f)$. Such a description requires **l**inear and **t**ime-**i**nvariant (LTI) systems. While the inverter is actually no LTI system due to the switching transistors, it appears predominantly linear for the high-frequency cancellation signal $v_{\mathrm{anti}}(t)$ because of the large input capacitance C_{in}. Therefore, calculations in frequency domain are viable and the propagation of the complex cancelling amplitudes $V_{\mathrm{anti}}(kf_0)$ to the sensor can be described by using $H_{\mathrm{anti}}^{\rightarrow\mathrm{sensor}}(kf_0)$:

$$V_{\mathrm{anti}}^{@\mathrm{sensor}}(kf_0) = H_{\mathrm{anti}}^{\rightarrow\mathrm{sensor}}(kf_0) \cdot V_{\mathrm{anti}}(kf_0) \quad (3)$$

C. Superposition of EMI and Anti-EMI at the Sensor

The superposition of EMI and anti-EMI at the sensing circuit must cause a destructive interference to suppress the disturbances at the critical interface port. Given that the cancellation is successful, it leads to a **res**idual EMI $V_{\mathrm{res}}^{@\mathrm{sensor}}(kf_0)$ according to (4):

$$V_{\mathrm{res}}^{@\mathrm{sensor}}(kf_0) = V_{\mathrm{EMI}}^{@\mathrm{sensor}}(kf_0) + \underbrace{H_{\mathrm{anti}}^{\rightarrow\mathrm{sensor}} \cdot V_{\mathrm{anti}}}_{=V_{\mathrm{anti}}^{@\mathrm{sensor}}(kf_0)} \quad (4)$$

D. Calculation of the Ideal Anti-EMI

For an ideal cancellation, the residual EMI picked up by the sensor should equal 0 V:

$$0\ \mathrm{V} = V_{\mathrm{EMI}}^{@\mathrm{sensor}}(kf_0) + H_{\mathrm{anti}}^{\rightarrow\mathrm{sensor}}(kf_0) \cdot V_{\mathrm{anti}}(kf_0) \quad (5)$$

So, the complex amplitudes $V_{\mathrm{anti}}(kf_0)$ of the required cancellation signal can be found by (6):

$$\overset{(5)}{\Rightarrow} V_{\mathrm{anti}}(kf_0) = -\frac{V_{\mathrm{EMI}}^{@\mathrm{sensor}}(kf_0)}{H_{\mathrm{anti}}^{\rightarrow\mathrm{sensor}}(kf_0)} \quad (6)$$

Even though the calculation of the required cancellation signal is -in theory- relatively simple, a realization is not trivial. The frequency spacing f_0 is often very small leading to an extremely high number of harmonics in a given frequency range. So, a very large number of complex amplitudes must be precisely identified. In the following, a suitable method is presented to solve this problem.

IV. FFT Method for Cancellation Signal Determination and Generation

In this chapter, a suitable method for the determination and generation of the cancellation signal is derived that is fundamentally based on a **f**ast **F**ourier **t**ransform (FFT). At first, the hardware for a digital active EMI cancellation system is introduced. Afterward, the developed algorithm is presented.

A. Digital Hardware of the Active EMI Cancellation System

The digital hardware setup required for the FFT method is depicted in Fig. 3. The sensing of the disturbances can be done by using an **a**nalog-to-**d**igital **c**onverter (ADC) and a memory unit. The acquired signal is passed to a signal processor running the FFT method described in the following section. The found cancellation signal is passed to another memory unit and injected into the system by using a **d**igital-to-**a**nalog **c**onverter (DAC). Signal injection and acquisition must be done in synchronicity with the EMI and, therefore, with the motor inverter. If the motor inverter and active EMI cancellation system are built into the same device (and ideally also controlled by the same digital hardware), the synchronous operation can usually easily be maintained.

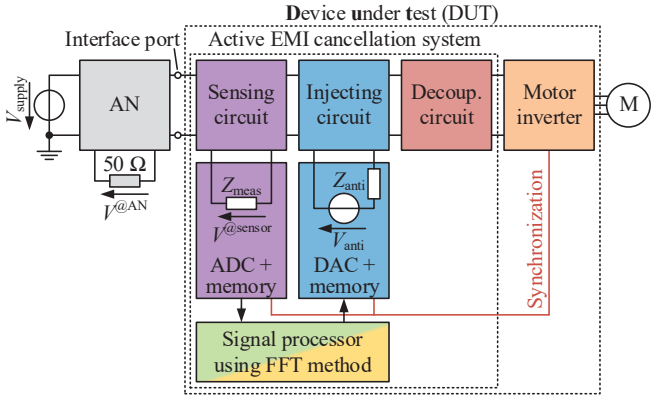

Fig. 3: Hardware setup for the complete system using the FFT method.

B. Algorithm

The goal of the FFT method is to find the right cancellation signal to suppress the disturbances of the motor inverter. If the complex amplitudes $V_{\mathrm{anti}}(kf_0)$ are known, the time-domain signal $v_{\mathrm{anti}}(t)$ can be found by using (2) or an IFFT (**i**nverse **f**ast **F**ourier **t**ransform). Since $V_{\mathrm{anti}}(kf_0)$ can be found by (6), only the complex amplitudes $V_{\mathrm{EMI}}^{@\mathrm{sensor}}(kf_0)$ and the transfer function $H_{\mathrm{anti}}^{\rightarrow\mathrm{sensor}}(kf_0)$ must be identified. The developed algorithm of the FFT method is visualized in Fig. 4 and explained in the following.

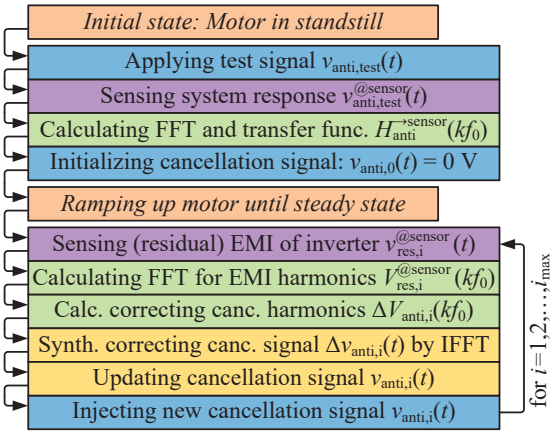

Fig. 4: Flowchart of the algorithm.

1) Initial State: Motor in Standstill

In the initial state, the motor inverter is in standstill (i.e. all control signals deactivated). In this state, the transfer function $H_{\mathrm{anti}}^{\rightarrow\mathrm{sensor}}(kf_0)$ can easily be identified by injecting a test signal $v_{\mathrm{anti,test}}(t)$ with arbitrary harmonics $V_{\mathrm{anti,test}}(kf_0)$. Due to the potentially small spacing f_0, the number of

harmonics may be inconveniently high. To resolve this issue, it is possible to use a larger frequency spacing and to interpolate between the test harmonics. The system's response $v_{\mathrm{anti,test}}^{@\mathrm{sensor}}(t)$ is acquired by the sensor. By applying an FFT, the complex amplitudes $V_{\mathrm{anti,test}}^{@\mathrm{sensor}}(kf_0)$ are found. The transfer function $H_{\mathrm{anti}}^{\rightarrow\mathrm{sensor}}(kf_0)$ can now be calculated by (7):

$$\overset{(3)}{\Rightarrow} H_{\mathrm{anti}}^{\rightarrow\mathrm{sensor}}(kf_0) = \frac{V_{\mathrm{anti,test}}^{@\mathrm{sensor}}(kf_0)}{V_{\mathrm{anti,test}}(kf_0)} \tag{7}$$

Afterward, the cancellation signal $v_{\mathrm{anti,0}}(t)$ is initialized with constant 0 V and the motor is ramped up until its final steady state.

2) Steady State: Motor in Stationary Operation with Periodic Control Signals

The following steps can be applied iteratively to optimize the cancellation signal $v_{\mathrm{anti,i}}(t)$ and to improve the cancellation result. At first, the sensor measures the superposition $v_{\mathrm{res,i}}^{@\mathrm{sensor}}(t)$ of EMI and anti-EMI for one or multiple periods T_0. Note that $v_{\mathrm{res,1}}^{@\mathrm{sensor}}(t)$ equals $v_{\mathrm{EMI}}^{@\mathrm{sensor}}(t)$ in the first iteration ($i = 1$) since the cancellation signal $v_{\mathrm{anti,0}}(t)$ is initialized with constant 0 V. By applying an FFT, the disturbing harmonics $V_{\mathrm{res,i}}^{@\mathrm{sensor}}(kf_0)$ are found. In analogy to (6), the complex amplitudes $\Delta V_{\mathrm{anti,i}}(kf_0)$ to cancel out the residual EMI $V_{\mathrm{res,i}}^{@\mathrm{sensor}}(kf_0)$ can be found by (8):

$$\overset{(6)}{\Rightarrow} \Delta V_{\mathrm{anti,i}}(kf_0) = -\frac{V_{\mathrm{res,i}}^{@\mathrm{sensor}}(kf_0)}{H_{\mathrm{anti}}^{\rightarrow\mathrm{sensor}}(kf_0)} \tag{8}$$

The time-domain signal $\Delta v_{\mathrm{anti,i}}(t)$ is synthesized by an IFFT. The previous cancellation signal $v_{\mathrm{anti,i-1}}(t)$ must be added since $\Delta v_{\mathrm{anti,i}}(t)$ is only a correction to suppress the residual EMI $v_{\mathrm{res,i}}^{@\mathrm{sensor}}(t)$:

$$v_{\mathrm{anti,i}}(t) = v_{\mathrm{anti,i-1}}(t) + \Delta v_{\mathrm{anti,i}}(t) \tag{9}$$

The found cancellation signal $v_{\mathrm{anti,i}}(t)$ is written into the injector's memory unit. The DAC repeatedly injects this signal into the system.

V. Demonstrator Results

In this chapter, demonstrator results are presented. At first, the goal is defined. The test setup and the realized DUT are introduced. The measurement results of the average and peak EMI reductions are presented and discussed. Last, the power of the generated cancellation signal is estimated.

A. Goal

The goal of this demonstration is to suppress the DM EMI at the DC input of a GaN motor inverter for frequencies of up to 30 MHz. Since the switching frequency f_{sw} is chosen to 100 kHz, the active EMI suppression is started at 50 kHz. The frequency f_{elec} of the three-phase system is chosen to 50 Hz. The here used motor has a pole pair number p of 4. So, the harmonics will have a spacing of $f_0 = 50\ \mathrm{Hz}/4 = 12.5\ \mathrm{Hz}$. Considering the frequency range from 50 kHz to 30 MHz, there will be $(30\ \mathrm{MHz} - 50\ \mathrm{kHz})/12.5\ \mathrm{Hz} + 1 \approx 2.4$ million harmonics that must be actively cancelled out.

B. Test Setup and DUT

The schematics of the complete test setup can be found in Fig. 5. A photograph of the overall test setup and the DUT can be found in Fig. 6 and Fig. 7, respectively.

The motor inverter is realized by three GaN half bridges EPC9033 from EPC and some large electrolyte capacitors to stabilize the input voltage. The supply voltage is 48 V. The motor is a synchronous machine. The control signals are generated by an HDAWG8 from Zurich Instruments. During startup, the electrical frequency f_{elec} of the three-phase system is ramped up until 50 Hz. After reaching 50 Hz, the control signals are periodically repeated. The motor is operated without mechanical load. However, there are phase currents of up to 30 A resulting in significant disturbances at the AN. To avoid that high-level disturbances of the three-phase system couple into the supply line between DUT and AN, the inverter is built into a closeable metal box, the motor lines are shielded by a metal coat and the motor is placed inside of a metal box. Additionally, the supply line between DUT and AN is shielded by copper tape.

The HDAWG8 is also used to generate the cancellation signal. Since frequencies of up to 30 MHz should be actively suppressed, the sampling rate of the device is set to 64 MS/s (Nyquist–Shannon sampling theorem). To avoid an increase of higher harmonics due to alias effects, a **l**ow-**p**ass **f**ilter (LPF) with a cutoff frequency of 32 MHz is applied in series.

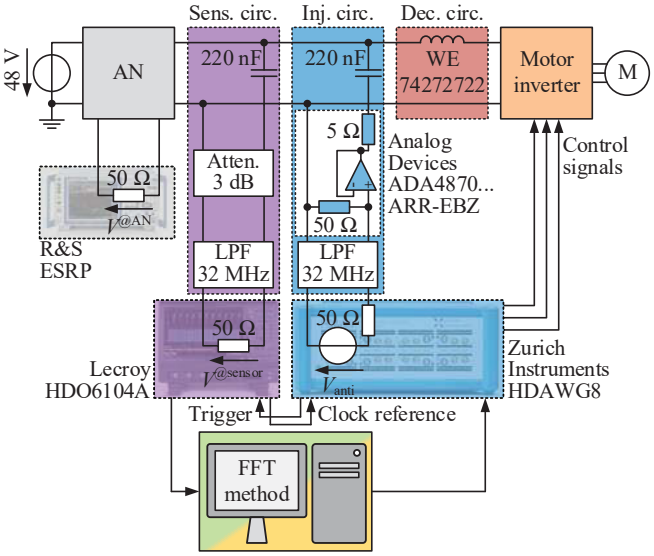

Fig. 5: Schematic of the realized test setup.

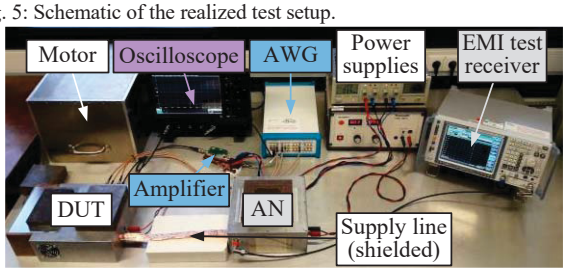

Fig. 6: Photograph of the realized test setup.

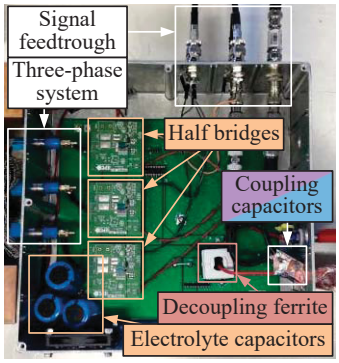

Fig. 7: Photograph of the realized DUT.

In this setup, a capacitive injector is chosen. The inverter has a much lower input impedance than the AN (seen by the injecting circuit) due to its stabilizing capacitors (note Fig. 1). Therefore, most of the injected current would flow towards the motor inverter and not support the active cancellation at the AN. To resolve this issue, the high-frequency input impedance of the motor inverter is increased by a decoupling inductor 74272722 from **W**ürth **E**lektronik (WE). While the input impedance of the AN (seen by the injecting circuit) tends towards 50 Ω for high frequencies (a few MHz), it is actually very low for lower frequencies (e.g. 3 Ω at 100 kHz) [1]. To efficiently inject cancellation signals at low frequencies, the cancellation source and the coupling element must have a very low impedance. Since the HDAWG8's internal impedance of 50 Ω is relatively high, an operational amplifier board ADA4870ARR-EBZ from Analog Devices is used that has an internal impedance of only 5 Ω. In the non-inverting configuration used here, it offers an amplification by the factor 4.5. The 220 nF coupling capacitor has an impedance of approximately 7.2 Ω at 100 kHz that declines further for higher frequencies.

The measurement of the residual EMI is done by using a capacitive sensing circuit and an oscilloscope HDO6104A from Teledyne LeCroy with a termination impedance of 50 Ω. For a precise measurement of the disturbances, only the relevant frequency range is measured by using an LPF with a cutoff frequency of 32 MHz. This coupling is also realized by a 220 nF capacitor. To avoid resonances between the overall system and the LPF, a 3 dB attenuator (50 Ω) is installed in between. The oscilloscope rescales its vertical range in every iteration to maximize the measurement precision. Oscilloscope and AWG must be synchronized for the FFT method. For this purpose, the AWG sends a trigger signal to the oscilloscope. To avoid errors due to different clock rates, the AWG uses the reference clock signal of the oscilloscope.

Both oscilloscope and AWG are controlled by a PC with MATLAB. The oscilloscope measures one complete period of the disturbances ($T_0 = 1/f_0 = 1/12.5\,\text{Hz} = 80\,\text{ms}$). Since it operates with a sampling rate of 250 MS/s, 20 million samples are acquired and send to the PC. The PC uses the FFT method of Section IV.B to calculate the required cancellation signals (also with the length of $T_0 = 80$ ms) to suppress the ~2.4 million harmonics. Since the HDAWG8 is operated with a sampling rate of 64 MS/s, the cancellation signal consists of approximately 5.1 million samples. This signal is transferred to the AWG and injected into the system.

C. Measured EMI Reduction (at the Artificial Network)

The achieved EMI suppression in the frequency range from 50 kHz to 30 MHz is evaluated by an ESRP EMI test receiver from Rohde & Schwarz at the AN. It is set up in reference to the automotive standard CISPR 25 [1] with a **r**esolution **b**and**w**idth (RBW) of 9 kHz, a measurement time of 160 ms (two periods of disturbances) and a frequency step of 2.25 kHz. To measure the spectrum in a reasonable time, the FFT-based time domain scan is used. The disturbances are evaluated by using the average or peak detector.

Note that the cancellation system introduces some passive attenuation due to the injecting, sensing and decoupling circuits, and an active suppression due to the injected cancellation signals. To investigate the performance of the FFT method, only the active suppression shall be measured. Therefore, the reference measurements are the disturbances with the already installed (but deactivated) cancellation system. The EMI reductions found in the following are solely the active suppression resulting from the injected signals after the respective iteration of the FFT method.

The measurement results for the average detector are depicted in Fig. 8. After the first iteration of the algorithm, the first switching harmonic at 100 kHz is suppressed by 25 dB. The tenth switching harmonic at 1 MHz is even suppressed by over 32 dB. However, the achieved reduction declines for higher frequencies. By doing multiple iterations, the algorithm improves the cancellation result. After the seventh iteration, the EMI is suppressed by over 48 dB at 100 kHz, by up to 54 dB between 200 and 500 kHz, and by over 27 dB at 30 MHz.

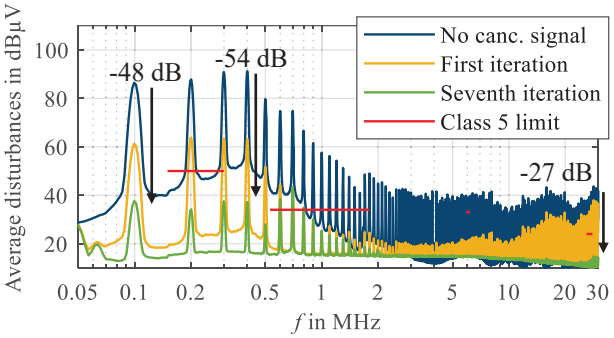

Fig. 8: Average disturbances measured by the EMI test receiver at the AN.

For reference, the strictest limit (class 5) of the CISPR 25 [1] is also given in Fig. 8. It can be found that the inverter fulfills this limit in the complete frequency range except for 600, 700 and 800 kHz. While the reason for this issue could not be finally identified yet, it is suspected that the oscilloscope measurement may be distorted by, e.g., unintended ground loops of the extensive test setup. This problem may be solved by a more sophisticated ground concept of the motor inverter and the cancellation system.

The measurement results for the peak detector are presented in Fig. 9. Since the duty cycles of the control signals vary with the three-phase system's frequency f_{elec} of 50 Hz, the peak disturbances are higher than the average. The EMI reduction found by the peak detector is very similar to the one found by the average detector. So, the active cancellation system reliably cancels out the EMI. Since the class 5 limit is higher for the peak disturbances, it is already fulfilled.

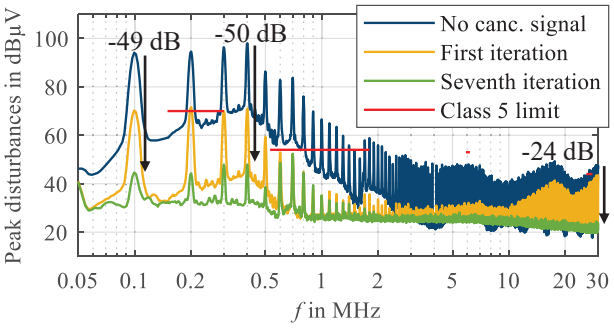

Fig. 9: Peak disturbances measured by the EMI test receiver at the AN.

Considering the discontinuous limit lines of the standard CISPR 25 [1], it can be found that it is actually not necessary to suppress the harmonics in the complete frequency range. For compliance, it would be sufficient to only suppress the harmonics in the restricted frequency bands. Since the proposed algorithm selectively suppresses each harmonic by a respective cancellation since wave, it can easily be limited to the relevant frequency bands. By doing so, the number of

considered harmonics can be reduced from 2.4 million below 300.000. This measure can help to significantly reduce the required computation effort of the cancellation system. Such a technique has been demonstrated for a DC-to-DC converter in [16].

D. Power of the Generated Cancellation Signal

The signal internally generated by the operational amplifier board ADA4870ARR-EBZ has an RMS (**r**oot **m**ean **s**quare) value of approximately 178 mV. The corresponding power depends on the impedance seen by the internal voltage source. Since the impedances of the injecting circuit, sensing circuit, decoupling circuit and overall system are not identified, they are assumed to be $0\,\Omega$ for a worst-case approximation. So, all the generated voltage drops over the amplifier board's output impedance of $5\,\Omega$. The power can be estimated to $(178\,\mathrm{mV})^2/5\,\Omega \approx 6.3\,\mathrm{mW}$. Considering the high DC voltage of 48 V, the high motor currents of up to 30 A and a DC input power of approximately 86 W, the power of the cancellation signal is negligible. There are two reasons: First, the EMI is widely attenuated by the stabilizing capacitors at the input of the inverter. So, the EMI has only a small power content. Second, there is an effective coupling of the cancellation source to the overall system with only little transfer losses. Due to these two effects, the power of the required cancellation signal is also small.

VI. Conclusion and Outlook

In this contribution, the periodic DM EMI of a GaN-based motor inverter is actively cancelled out by injecting synthesized and synchronized cancellation signals. Since the disturbances consist of approximately 2.4 million harmonics in the considered frequency range (50 kHz – 30 MHz), it was required to synthesize the cancellation signal from the same number of sine waves. An appropriate algorithm using an FFT and some calculations in frequency domain has been presented. The algorithm has been applied to a prototype test setup consisting of an oscilloscope, an arbitrary waveform generator, a PC and some analog components. The average and peak disturbances have been successfully suppressed by, e.g., 48 dB at 100 kHz, 54 dB at 400 kHz and 27 dB at 30MHz. While the peak emissions already fulfill the strictest limit (class 5) of the automotive standard CISPR 25 [1], the average emissions are too high for the frequencies of 600, 700 and 800 kHz. An optimized test setup may help to resolve this problem. The power of the generated cancellation signal has been estimated to be below 6.3 mW although there are large currents in the three-phase system of up to 30 A.

All in all, the proposed method has shown to be very effective in suppressing periodic DM EMI of a motor inverter. Due to the high EMI reduction, the size of passive filters may be significantly reduced. The high-end laboratory setup used here is obviously no feasible solution for practical realizations due to its large size and high cost. Since the required functionality is not too complex (FFT, adjustments in amplitude and phase, IFFT), it may be realized by integrated circuits at significantly lower costs in the future.

Currently, an optimized design of the inverter is being built. This redesign may help to reduce the remaining disturbances at 600, 700 and 800 kHz. Furthermore, investigations at higher transfer powers are planned. Due to the larger input currents, a compact design of the inductive decoupling element can be expected to be more challenging in this case.

Acknowledgment

The work presented in this paper was partially funded by the German Federal Ministry of Education and Research (BMBF) as part of the project RobKom ("**Rob**uste **Kom**munikation in autonomen Elektrofahrzeugen") with the grant number 16EMO0380. The responsibility for this publication is held by the authors only.

References

[1] CISPR 25 – *Vehicles, boats and internal combustion engines – Radio disturbance characteristics – Limits and methods of measurement for the protection of on-board receivers*, 4th ed., Feb. 2015.

[2] P. Lueg, "Process of silencing sound oscillations," U.S. Patent 2 043 416, Jun. 9, 1936.

[3] S. Feng, W. Sander, T. Wilson, "Small-capacitance nondissipative ripple filters for dc supplies," *IEEE Trans. Magn.*, vol. 6, no. 1, pp. 137-142, Mar. 1970.

[4] J. Walker, "Designing practical and effective active EMI filters," in Proc. *Powercon 11 Conf.*, Dallas, Texas, USA, 10-12 Apr. 1984, Paper I-3.

[5] L. E. LaWhite and M. F. Schlecht, "Active filters for 1-MHz power circuits with strict input/output ripple requirements," *IEEE Trans. Power Electron.*, vol. PE-2, no. 4, pp. 828-290, Oct. 1987.

[6] L. E. LaWhite, M. F. Schlecht, "Design of active ripple filters for power circuits operating in the 1-10 MHz range," *IEEE Trans. Power Electron.*, vol. 3, no. 3, pp. 310-317, Jul. 1988.

[7] N. K. Poon, J. C. P. Liu, C. K. Tse, M. H. Pong, "Techniques for input ripple current cancellation: classification and implementation [in smps]," *IEEE Trans. Power Electron.*, vol. 15, no. 6, pp. 1144-1152, Nov. 2000.

[8] Y.-C. Son, S.-K. Sul, "Generalization of active filters for EMI reduction and harmonics compensation," *IEEE Trans. Ind. Appl.*, vol. 42, no. 2, pp. 545-551, Mar./Apr. 2006.

[9] D. Hamza, M. Pahlevaninezhad, P. K. Jain, "Implementation of a novel digital active EMI technique in a DSP-based dc-dc digital controller used in electric vehicle (EV)," *IEEE Trans. Power Electron.*, vol. 28, no. 7, pp. 3126-3137, Jul. 2013.

[10] J. Ji, W. Chen, X. Yang, J. Lu, "Delay and decoupling analysis of a digital active EMI filter used in arc welding inverter," *IEEE Trans. Power Electron,* vol. 33, no. 8, pp. 6710-6722, Aug. 2018.

[11] Y.-C. Son and S.-K. Sul, "A new active common-mode EMI filter for PWM inverter," *IEEE Trans. Power. Electron.*, vol. 18, no. 6, pp. 1309–1314, Nov. 2003.

[12] W. Chen, X. Yang, and Z.Wang, "A novel hybrid common-mode EMI filter with active impedance multiplication," *IEEE Trans. Ind. Electron.*, vol. 58, no. 5, pp. 1826–1834, May 2011.

[13] S. Wang, Y. Y. Maillet, F. Wang, D. Boroyevich, and R. Burgos, "Investigation of hybrid EMI filters for common-mode EMI suppression in a motor drive system," *IEEE Trans. Power. Electron.*, vol. 25, no. 4, pp. 1034–1045, Apr. 2010.

[14] M. L. Heldwein, H. Ertl, J. Biela, and J. W. Kolar, "Implementation of a transformerless common-mode active filter for offline converter systems," *IEEE Trans. Ind. Electron.*, vol. 57, no. 5, pp. 1772–1786, May 2010.

[15] A. Bendicks, S. Frei, "Broadband Noise Suppression of Stationary Clocked DC/DC Converters by Injecting Synthesized and Synchronized Cancellation Signals," *IEEE Trans. Power Electron.*, vol. 34, no. 11, pp. 10665-10674, Jan. 2019.

[16] A. Bendicks, T. Osterburg, S. Frei, M. Wiegand, and N. Hees, "Wide-frequency EMI suppression of stationary clocked systems by injecting successively adapted cancellation signals," *in Proc. Int. Symp. Electromagn. Compat. Eur.*, Barcelona, Spain, 2-6 Sep. 2019, pp. 36–41.

[17] A. Bendicks, M. Gerten, S. Frei, "Aktive Unterdrückung der elektromagnetischen Störungen eines stationär betriebenen Antriebswechselrichters mithilfe von synthetisierten und synchronisierten Gegenstörsignalen," *in Proc. Conf. Electromagn. Compat.*, Cologne, Germany, Mar. 17-19, 2020.

[18] C. R. Paul, Introduction to Electromagnetic Compatibility, 2nd ed., Hoboken, NJ, USA: Wiley, 2006.